Acta Crystallographica Section D
Biological Crystallography
ISSN 0907-4449

Lessons from an aged, dried crystal of T_6 human insulin

G. David Smith[a,b]* and Robert H. Blessing[b,c]

[a]Structural Biology and Biochemistry, Hospital for Sick Children, 555 University Avenue, Toronto, Ontario M5G 1X8, Canada, [b]Hauptman–Woodward Medical Research Institute, 73 High Street, Buffalo, NY 14203, USA, and [c]Department of Structural Biology, School of Medicine and Biomedical Sciences, State University of New York at Buffalo, USA

Correspondence e-mail: gdsmith@sauron.psf.sickkids.on.ca

Received 7 April 2003
Accepted 27 May 2003

PDB References: 100 K T_6 insulin, 1os3, r1os3sf; 295 K T_6 insulin, 1os4, r1os4sf.

Dedicated to Drs Ronald E. Chance and Bruce H. Frank, now retired from Lilly Research Laboratories, where they were pioneers in the development of the production of biosynthetic human insulin.

The structure of the T_6 hexameric form of human insulin has been determined at both room temperature and 100 K from a single air-dried crystal. At 100 K, the space group is *R*3 and the asymmetric unit consists of a dimer, as has been observed previously in hydrated structures. At room temperature, the space group is *P*1 and the unit cell contains a quasi-threefold-symmetric hexamer. In the absence of stabilizing water interactions, the N-termini of all six A chains in the room-temperature structure appear to have undergone partial unfolding, but the N-termini of these chains are well ordered in the 100 K structure. Other differences between the room-temperature and 100 K structures involve the coordination around the zinc ions. At 100 K, both zinc ions clearly exhibit dual coordination: zinc is octahedrally coordinated in one half of the zinc sites but tetrahedrally coordinated in the other half; at room temperature, the electron densities suggest tetrahedral coordination but the bond distances to the fourth ligands are longer than expected. Contrary to what has been observed to date in all other T_6 insulin structures, there are no contacts between pairs of GluB13 residues, either at room temperature or at 100 K, that would suggest the presence of a hydrogen bond. At room temperature, three of the six independent GluB13 side chains are disordered; at 100 K, both independent side chains are disordered. The disorder in the GluB13 side chains and the lack of contacts between carboxylate groups suggests that as a result of disruption of the hydration structure in the central core of the hexamer, all six B13 carboxylates bear a negative charge. This in turn suggests that in the hydrated structures the well ordered water structure in the central core is involved in stabilizing the B13 side-chain conformations and modulating charge repulsions among the six B13 glutamates if they are not protonated, or that, as is considered more likely, the water structure plays an important role in modulating the pK_a values of the B13 glutamates, resulting in protonation and hydrogen-bond formation.

1. Introduction

1.1. Insulin crystallography

Insulin is a polypeptide hormone that is synthesized, stored and secreted by the β cells in the pancreas. The hormone circulates in the bloodstream as a monomer which, when it interacts with its receptor, initiates a signal transduction cascade that ultimately results in the absorption and metabolism of glucose. The insulin monomer contains a 21-residue A chain and a 30-residue B chain; the two chains are cross-linked by two disulfide bonds, while a third, intra-chain, disulfide bond links residues A6 and A11.

The crystal structure of insulin was first described by Adams *et al.* (1969), who showed that insulin crystallizes in the rhombohedral space group *R*3 and that an insulin dimer is the asymmetric unit in a threefold symmetric insulin hexamer. This form of insulin was originally called 2Zn insulin since two zinc ions are bound by the hexamer. In a second crystalline form of hexameric insulin, originally called 4Zn insulin, the N-termini of three of the six B chains were shown to have undergone a conformational change from extended to α-helical and in this altered conformational state the hexamer was found to have bound four zinc ions (Bentley *et al.*, 1976). Subsequently, further hexameric forms of insulin were discovered (Derewenda *et al.*, 1989) and a T/R conformational notation was introduced (Kaarsholm *et al.*, 1989) according to which T-state monomers have an extended conformation and R-state monomers have an α-helical conformation in the first eight residues of the B chain. Later, the notation R^f was introduced to denote an R-state monomer with a 'frayed' α-helical conformation, in which residues B1–B3 are extended (Ciszak *et al.*, 1995).

In T_6 hexameric insulin, cryocooling has been shown to produce a displacement of approximately 8 Å at the N-terminus of one of the B chains (Smith *et al.*, 2003). In cryocooled $T_3R_3^f$ insulin crystals, a phase change occurs in which the *c* axis is doubled, producing two independent TR^f dimers in the asymmetric unit (Smith *et al.*, 2001). Accompanying this phase change is the generation of two additional zinc ion-binding sites between the two independent hexamers. Thus, the molecular and crystal structure of hexameric insulin responds not only to the addition of reagents that induce allosteric conformational transformation but also to changes in temperature.

The complete description of the T_6 (2Zn) porcine insulin structure at 1.5 Å resolution by Baker *et al.* (1988) showed that the conformations of the two crystallographically independent monomers in the hexamer are nearly identical. Each A chain consists of a central extended segment of polypeptide chain flanked by two α-helical segments, while each B chain consists of a central α-helical segment flanked by two segments with extended conformations. Two zinc ions lie on the crystallographic threefold axis, some 16 Å apart, on opposite sides of the hexamer and each zinc ion is octahedrally coordinated by $N^{\epsilon 2}$ atoms of three symmetry-related HisB10 side chains and three symmetry-related water molecules. A joint X-ray/neutron refinement has also been reported for the T_6 porcine insulin hexamer (Wlodawer *et al.*, 1989). More recently, the structure of the T_6 human insulin hexamer has been analyzed at 1.0 Å resolution with X-ray data measured at a temperature of 120 K (Smith *et al.*, 2003). All the earlier insulin crystal structure analyses were based on room-temperature diffraction data.

Insulin also forms zinc-free cubic crystals which contain a monomer in the asymmetric unit and which have also been studied extensively by crystallographic techniques. Diao (2003) has examined the structural changes which occur by determining ten cubic insulin structures in the pH range 5.0–9.0. Badger (1993) has observed multiple hydration layers in the solvent-rich cubic insulin crystals (60% solvent by volume) by performing iterative refinement of the solvent density model; although the densities were not interpretable in terms of an atomic water-structure model, the reduction in $R_{\rm free}$ was significant.

1.2. Protein crystal dehydration

Controlled dehydration of monoclinic lysozyme crystals to 88% relative humidity results in a phase change in which two molecules which were independent in the unit cell of the fully hydrated crystal become related by a crystallographic twofold screw axis in the dehydrated crystal (Madhusudan *et al.*, 1993). The dehydrated crystals had a solvent content of 22% by volume and diffracted to 1.75 Å resolution using a 4 kW sealed-tube copper X-ray source and photographic methods to record diffraction data. The overall backbone conformation was found to be very similar in the hydrated and dehydrated crystals, with r.m.s. differences of the order of 0.7 Å.

The structure of severely desiccated crystals of form IX of bovine pancreatic ribonuclease A has also been reported (Bell, 1999) with desiccation times of 2.5 and 4 d. In these experiments, the crystal was placed in a sealed glass capillary with one end packed with Drierite. Diffraction data were measured to a resolution of 1.9 Å with synchrotron radiation and a comparison of the desiccated and hydrated structures (Dung & Bell, 1997) revealed an r.m.s. displacement of main-chain atoms of 1.6 Å.

Controlled dehydration of protein crystals has been shown in some cases to increase the resolution to which the proteins diffract (Heras *et al.*, 2003, and references therein). In the case of DsbG, a member of the disulfide-bond family of proteins, reducing the solvent content of the crystals eliminated streaky spots and increased the resolution from 10 to 2 Å.

Diffraction patterns from air-dried insulin crystals have been used to obtain unit-cell dimensions (Schlichtkrull, 1958), but no further studies have been reported on dehydrated insulin crystals. Reported herein is the structure of T_6 human insulin at room temperature and at 100 K from a single crystal air-dried at room temperature.

2. Experimental

2.1. Crystallization

Crystals of T_6 human insulin were grown in batch mode in microgravity aboard the US NASA space shuttle flight STS-86 in September–October 1997 using the UAB PCF (University of Alabama at Birmingham Protein Crystallization Facility) apparatus. Biosynthetic human insulin complexed with zinc was supplied by Lilly Research Laboratories. Buffers, salts and other reagents were purchased and used without further purification. The crystallizing media consisted of 5 mg ml^{-1} insulin, 0.01 *M* HCl, 0.007 *M* zinc acetate, 0.05 *M* sodium citrate and 17% acetone at a pH of 6.3. The microgravity-grown crystals were large, well shaped and free of inclusions.

Table 1
Data-measurement statistics for dehydrated T_6 human insulin at 295 and 100 K.

	295 K	100 K
Space group	*P*1	*R*3
Unit-cell parameters†		
a (Å)	33.90 (49.06)	81.51 (48.39)
b (Å)	49.44 (49.44)	81.51 (48.39)
c (Å)	49.26 (49.26)	33.76 (48.39)
α (°)	115.12 (115.12)	90.0 (114.76)
β (°)	104.01 (114.14)	90.0 (114.76)
γ (°)	102.69 (115.45)	120.0 (114.76)
Unit-cell volume per monomer (Å^3)	11244	10792
Overall B_{iso} (Å^2)	42.71	33.4
Resolution (Å)	41.64–2.25	16.42–1.95
Total data	15512	22524
Unique data	10252	6070
Average redundancy	1.5	3.7
Completeness (%)	82.7	99.6
Overall R_{merge}	0.070	0.045
$\langle F^2\rangle/\langle\sigma(F^2)\rangle$	7.3	15.9
Final shell		
Resolution (Å)	2.33–2.25	2.02–1.95
Completeness (%)	85.9	100.0
R_{merge}	0.289	0.175
$\langle F^2\rangle/\sigma\langle(F^2)\rangle$	1.6	3.67

† The pseudo-rhombohedral (295 K) setting and rhombohedral (100 K) setting unit-cell parameters are given in parentheses.

2.2. Diffraction measurements

X-ray diffraction measurements were made with Cu $K\alpha$ radiation using a laboratory diffraction apparatus equipped with a Rigaku RU-H3R rotating-anode generator, Osmic confocal diffraction mirrors, an MSC Xtreme cryotemperature device and a Rigaku R-AXIS IV^{++} imaging-plate detector system. The program *CrystalClear* was used to obtain preliminary unit-cell parameters, to determine the space group and to record the diffraction images; integration, scaling and merging of the data were performed using the *d*TREK* program (Pflugrath, 1999). The resulting independent data were further processed to reorder and reformat the data using the program *SORTAV*, to improve weak data using the program *BAYES* and to obtain estimates of the absolute scale factor and overall isotropic temperature factor using the program *LEVY* (Blessing, 1997, 1999; Blessing *et al.*, 1998; French & Wilson, 1978).

The crystal used for the present work was a rhomboid-shaped crystal, 0.84 mm long and 0.26 mm thick, that originally had been cryoprotected, looped, flash-frozen and stored in a liquid-nitrogen Dewar in March 1998. Cryoprotection was provided by 60% mother liquor plus 25% glycerol and 15% PEG 300 (by volume) as described previously (Smith *et al.*, 2003). The crystal was one of several specimens prepared for diffraction measurements, but was not one of the specimens used for the measurements and was therefore left in the liquid-nitrogen storage Dewar. During the holidays in December 2001, the temperature sensor in the Dewar malfunctioned and all the stored samples warmed to room temperature. When this was discovered, the mounted insulin crystal was put aside on a shelf in an air-conditioned laboratory, where it remained exposed to the ambient environment for approximately six months. Thereafter, during a search for a crystal-mounting pin, the aged, dried crystal was rediscovered and microscopic examination revealed not only that the crystal was still attached to the loop, but also that the crystal had maintained its integrity and was still clear and transparent. Apparently, a clear PEG–glycerol–solutes skin had formed and cemented the crystal in its mounting loop when the cryoprotected mother liquor that coated the crystal evaporated to dryness. Given these surprising results, a 5 min X-ray exposure showed that the crystal still diffracted to a resolution of approximately 2.0 Å at room temperature. Because of concern that the crystal might be dislodged from the loop or crack if cryofreezing were attempted, initial diffraction experiments were performed at room temperature. Following indexing of an initial image and refinement of the unit-cell parameters, the apparent space group was determined to be *R*3, with unit-cell parameters $a = 82.39$, $c = 34.10$ Å, values that are consistent with the room-temperature structure of T_6 hexameric insulin. 240 frames of data were recorded with φ = 0–120° and $\Delta\varphi = 0.5°$.

On completion of the room-temperature data measurement, the cryostream nozzle was moved into place and the crystal was flash-frozen at 100 K. The crystal appeared to suffer no damage upon cryofreezing and data measurement was initiated. Preliminary diffraction experiments indicated the space group to be *R*3, with unit-cell parameters $a = 81.46$, $c = 33.88$ Å. 240 frames of data were recorded with φ = 0–120° and $\Delta\varphi = 0.5°$.

The room-temperature and 100 K data sets were integrated, scaled and merged separately. The 100 K data presented no problems, but attempts to process the room-temperature data in space group *R*3 resulted in an R_{merge} of approximately 50%. Therefore, the room-temperature space group was reassigned as *P*1 and the frames were re-integrated, re-scaled and re-merged to give the entirely acceptable data statistics presented, along with the 100 K data statistics, in Table 1.

The hexagonal setting for space group *R*3 is typically used rather than the rhombohedral setting; the transformation of the hexagonal setting to the rhombohedral one is given by $a_r = 2/3a_h + 1/3b_h + 1/3c_h$, $b_r = -1/3a_h + 1/3b_h + 1/3c_h$ and $c_r = -1/3a_h - 2/3b_h + 1/3c_h$, where the subscripts '*r*' and '*h*' refer to rhombohedral and hexagonal settings, respectively. The triclinic unit cell of the room-temperature structure can also be transformed into a pseudo-rhombohedral setting by $a_{p\text{-}r} = a_t + b_t + c_t$, $b_{p\text{-}r} = -b_t$ and $c_{p\text{-}r} = -c_t$, where the subscripts '*p–r*' and '*t*' refer to pseudo-rhombohedral and triclinic, respectively. The unit-cell parameters for both the 100 K rhombohedral setting and the room-temperature pseudo-rhombohedral setting are included in Table 1 to make the relationship between the triclinic and rhombohedral unit cells apparent.

2.3. Structure solution and refinement

2.3.1. The room-temperature structure. An insulin hexamer was constructed from the dimer of PDB entry 4ins

(Baker *et al.*, 1988), excluding all water molecules and alternate side-chain orientations. The orientation of the hexamer within the triclinic unit cell was determined using the cross-rotation protocol as implemented in *CNS* (DeLano & Brünger, 1995) and the geometric center of the hexamer was then placed at the body center of the triclinic cell. Rigid-body refinement of the entire hexamer using data between 15.0 and 4.0 Å resolution resulted in a residual of 0.340. Treating each of the six monomers as a rigid body and the two zinc ions as an additional rigid body and using data between 42.0 and 2.5 Å resolution resulted in a residual of 0.348.

The refinement was continued with *CNS* using all data, applying an overall anisotropic temperature-factor correction and a bulk-solvent correction, and using maximum-likelihood torsion-angle dynamics, conjugate-gradient refinement and individual temperature-factor refinement (Rice & Brünger, 1994; Brünger *et al.*, 1998; Adams *et al.*, 1997; Pannu & Read, 1996). Bond distances involving the zinc ions were not restrained and non-crystallographic symmetry was not invoked. Approximately 10% of the data were reserved for cross-validation and were never used in the refinement (Brünger, 1992).

At the end of each round of refinement, σ_A-weighted $(2F_o - F_c)$ electron-density and $(F_o - F_c)$ difference electron-density maps (Read, 1986; Brünger *et al.*, 1997) were carefully examined using the graphics programs *CHAIN* (Sack, 1988) or *XtalView* (McRee, 1999). Adjustments of, additions to or deletions from the protein chains of the model were made and several water molecules were added, all in accord with good electron density. Particular difficulty was encountered in modeling the first five or six residues in each of the six A chains because the electron density in their neighborhoods was, in general, not continuous.

At the conclusion of the refinement, the model for the hexamer in the asymmetric unit in space group *P*1 consisted of 2268 protein atoms, two zinc ions and 16 water molecules. No electron density was observable for the six C-terminal ThrB30 residues. Other residues that were omitted from the final model include LysB29.2[1], LysB29.3, GlyA1.4, LysB29.4, LysB29.6 and LysB29.6. Owing to missing electron density for their side chains, GluB21.1, ArgB22.1, LysB29.1, AsnB3.2, GluB21.2, IleA2.3, GluB21.3, ArgB22.3, IleA2.4, ValA3.4, GluA4.4, GlnA5.4, GluB21.5, ArgB22.5 and GluB21.6 were truncated to alanine. No density was observable for the C^{δ}, $O^{\epsilon 1}$ and $O^{\epsilon 2}$ atoms of GluB13.3 and therefore these atoms were omitted from the model. The $(2F_o - F_c)$ electron density for the carboxylate groups of GluB13.1 and GluB13.2 was very weak and the side chains nearly interpenetrated; therefore, these side chains were assigned occupancies of 0.5. A total of 234 (93.2%), 15 (6.0%) and two (0.8%) of the non-glycine or non-proline residues lie in the most favored, additionally allowed or generously allowed regions of the Ramachandran plot, respectively, as determined by *PROCHECK* (Laskowski *et al.*, 1993); no residues lie within the disallowed region. Deviations of the torsion angles of SerA9 from the most favored regions of the Ramachandran plot have been observed in all T-state insulin monomers. SerA9.1 and SerA9.5 lie on the boundary of the additionally allowed and generously allowed regions, while SerA9.2, SerA9.3 and SerA9.4 lie within the additionally allowed region. Refinement statistics are given in Table 2.

[1] The decimal portion 0.1–0.6 in the residue number refers to the monomer number 1–6 in the asymmetric unit.

Table 2
Data-refinement statistics for dehydrated T_6 human insulin at 295 and 100 K.

Values in parentheses are for the highest resolution shell.

	295 K	100 K
No. of reflections	10239	6070
Resolution range (Å)	41.7–2.25 (2.39–2.25)	16.42–1.95 (2.07–1.95)
Completeness (%)	82.7 (86.2)	99.6 (100.0)
R value	0.243 (0.310)	0.216 (0.260)
$R_{\rm free}$ value	0.295 (0.376)	0.253 (0.339)
Cross-validated est. error (Å)	0.44	0.18
R.m.s. deviations from ideal		
Bond lengths (Å)	0.007	0.006
Bond angles (°)	1.2	1.1
Dihedral angles (°)	22.2	20.2
Improper angles (°)	0.81	0.67
Isotropic thermal model restraints (Å^2)		
Main-chain bonds	1.52	1.66
Main-chain angles	2.54	2.70
Side-chain bonds	1.94	2.05
Side-chain angles	2.78	3.13

2.3.2. The 100 K structure. Since the unit-cell parameters are nearly identical to those of the room-temperature T_6 insulin structure, the structure of PDB entry 4ins was used as a starting model following removal of all water molecules and alternate side-chain orientations. Using data between 15.0 and 4.0 Å resolution, rigid-body refinement treating the entire dimer as a single rigid body resulted in a residual of 0.323. A second round of rigid-body refinement using data between 16.5 and 2.5 Å resolution produced a residual of 0.346. The model was subjected to a cycle of torsion-angle refinement, conjugate-gradient refinement and individual temperature-factor refinement, which resulted in an *R* factor of 0.269 and an $R_{\rm free}$ of 0.310.

In the 120 K structure of hydrated T_6 human insulin, the first four residues of the B chain of monomer 2 are displaced relative to the room-temperature structure, resulting in a 7.86 Å shift of the C^{α} atom of PheB1.2 (Smith *et al.*, 2003). In the 100 K structure of the dried crystal, the $(2F_o - F_c)$ electron density in the vicinity of the first three residues of the B chain of monomer 2 was not as complete as in the rest of the protein, so rigid-body refinement was performed using the 120 K human insulin structure (PDB code 1mso) as a model. A cycle of torsion-angle refinement followed by conjugate-gradient and individual temperature-factor refinement resulted in an *R* factor of 0.283 and an $R_{\rm free}$ of 0.340. The increase in both *R* and $R_{\rm free}$ and the appearance of the σ_A-weighted $(2F_o - F_c)$ and $(F_o - F_c)$ electron-density maps clearly showed that the N-terminal B-chain residues of monomer 2 in the dried crystal at 100 K do not adopt the shifted conformation observed in the hydrated crystal at 120 K.

The refinement was continued using the protocol described above for the room-temperature structure. At the end of the refinement, the model for the dimer in the asymmetric unit in space group *R*3 consisted of 769 protein atoms, two zinc ions, two chloride ions and 40 water molecules. No density was observable for either of the C-terminal ThrB30 residues or for LysB29.2. In the absence of side-chain density, GluB21.1, ArgB22.1, LysB29.1 and GlnA5.2 were truncated to alanine. The side chain of SerA12.2 was modeled in two discrete orientations. Because of persistent $(2F_o - F_c)$ and $(F_o - F_c)$ densities corresponding to alternate C^γ positions, the side chains of GluB13.1 and GluB13.2 were also modeled in two orientations; however, no electron density was observable for the carboxylate group of the second conformation of GluB13.1 or for the carboxylate group of the two alternate side-chain conformations of GluB13.2. An analysis of the backbone torsion angles using *PROCHECK* (Laskowski *et al.*, 1993) shows that 78 (92.9%), five (6%) and one (1.2%) of the residues lie in the most favored, additionally allowed or generously allowed regions of the Ramachandran plot, respectively. SerA9.1 lies in the generously allowed region, while SerA9.2 lies in the additionally allowed region. Refinement statistics are presented in Table 2.

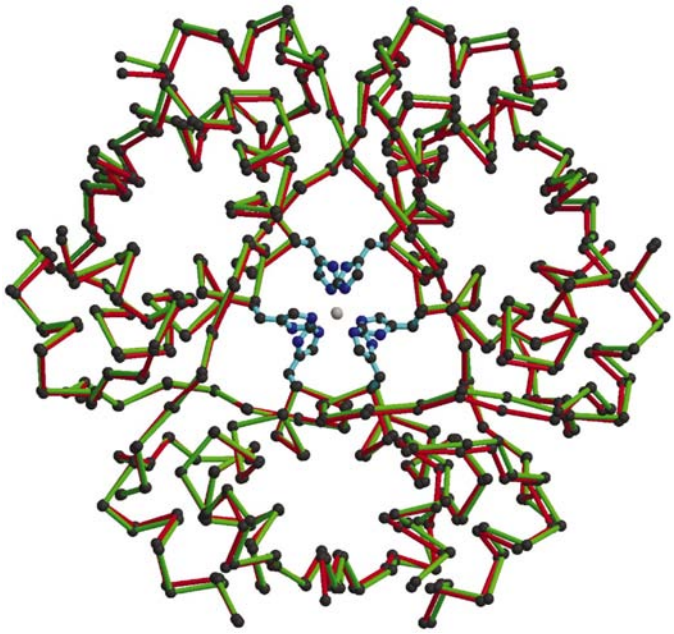

Figure 1
A C^α-trace superposition of the triclinic room-temperature (green) and trigonal 100 K (red) insulin hexamers as viewed along the pseudo-threefold and crystallographic threefold axes in the rhombohedral setting of the unit cells. For the sake of clarity, the zinc ion (gray) and HisB10 side chains (cyan) are only illustrated for the 100 K hexamer. This drawing was constructed by transforming the threefold-symmetric 100 K hexamer into the rhombohedral setting and then translating the center of gravity of the entire hexamer to the body center of the unit cell; the pseudo-symmetric room-temperature hexamer was transformed into the pseudo-rhombohedral setting and the center of gravity of the backbone atoms of B9–B19 of all six B chains was translated to the body center of the unit cell. This procedure ensures that the pseudo-threefold axis is aligned with the crystallographic threefold axis. Prepared with the programs *MOLSCRIPT* (Kraulis, 1991) and *Raster3D* (Merritt & Bacon, 1997).

3. Discussion

3.1. The room-temperature structure

Using the crystallization conditions described above, T_6 insulin usually crystallizes in space group *R*3, although on one occasion a triclinic crystal with unit-cell parameters nearly equal to those of the crystal of the present study was obtained (J. L. Whittingham & G. D. Smith, unpublished data), which can be transformed to a pseudo-rhombohedral unit cell as shown in Table 1. Although the unit-cell parameters obtained from the initial images were highly consistent with the

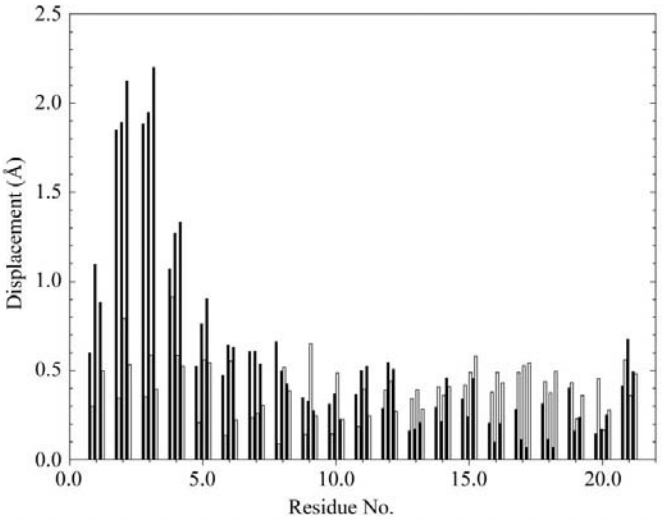

Figure 2
A-chain C^α displacements between the exactly threefold-symmetric hexamer constructed from PDB entry 4ins and the approximately threefold-symmetric hexamer in the triclinic room-temperature structure of the dried crystal in the present study. Black bars represent monomers 1, 3 and 5, while white bars represent monomers 2, 4 and 6. There is no bar plotted for GlyA1.3 because it could not be modeled in the present study.

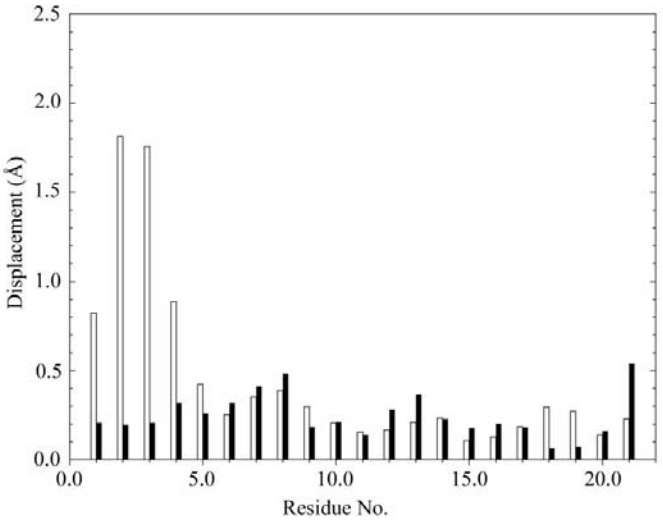

Figure 3
C^α displacements between the T_2 dimer A chains in the rhombohedral structure of the dehydrated crystal at 100 K from the present study and those from PDB entry 4ins. White bars represent monomer 1, while black bars represent monomer 2.

rhombohedral cell, changes in conformation that resulted from drying evidently deformed the exactly threefold symmetric hexamer to a quasi-threefold-symmetric hexamer.

As can be seen from the C^{α} trace in Fig. 1, where the local non-crystallographic threefold axis of the room-temperature triclinic structure is aligned with the crystallographic threefold axis of the 100 K trigonal structure, there does not appear to be a significant rotation of the pseudo-threefold axis from the crystallographic axis. However, there are small but numerous deviations of the C^{α} atoms from their threefold symmetric counterparts. As a measure of the departure from threefold symmetry in the room-temperature hexamer, displacements were calculated between 2221 pseudo-symmetrically related atoms. Respective mean and r.m.s. displacements were calculated to be 0.39 and 0.61 Å; 65 displacements exceed 2.0 Å, with the maximum being 4.16 Å. These distortions are sufficient to eliminate the threefold symmetry in space group *R*3 and revert to the lower symmetry space group *P*1.

An alignment of the deformed hexamer from the present study with the threefold-symmetric hexamer constructed from PDB entry 4ins, minimizing the displacements of all A11–A19 and B11–B19 backbone atoms by a least-squares optimization procedure (Smith, 1993), resulted in a mean displacement of 0.28 Å for the atoms used in the optimization and 0.44 Å for all backbone atoms. Most of the largest displacements occur at the N-termini of the A chains. With the exception of PheB1.2 and PheB1.4, with displacements of 1.59 and 1.03 Å, respectively, the displacements at the N-termini of the B chains are less than 0.52 Å.

In hydrated hexameric insulin crystal structures, the only protein–protein hydrogen-bonded interactions involving the first five residues of the A chains are those associated with the α-helical conformation; however, numerous water molecules participate in hydrogen-bonded interactions between these A-chain residues and a variety of B-chain residues. Crystal contacts play no role in the conformation of the first five residues of the A chain, as these residues make no contacts shorter than 3.8 Å to an adjacent hexamer. Illustrated in Fig. 2 are the displacements of the C^{α} atoms of all six A chains of the deformed hexamer relative to the C^{α} positions in the threefold-symmetric hexamer constructed from PDB entry 4ins. With the exception of the first five residues, the majority of the displacements are less than 0.5 Å. In trimer 1, which contains monomers 1, 3 and 5, all $3 \times 5 = 15$ C^{α} atoms of the first five residues are displaced by more than 0.5 Å from the corresponding C^{α} atoms of the symmetric hexamer and eight displacements exceed 1.0 Å. In contrast, only eight C^{α} displacements in trimer 2 exceed 0.5 Å, and none exceed 1.0 Å. The B-chain C^{α} displacements do not reflect this pattern.

The $(2F_o - F_c)$ electron density was particularly poor in the vicinity of the N-termini of the A chains in the dried crystal at room temperature, and this required elimination of one

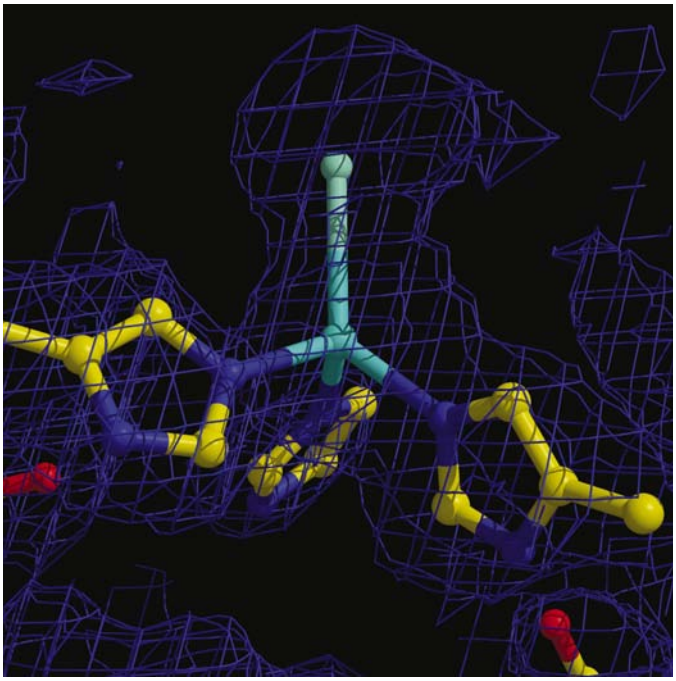

Figure 4
$(2F_o - F_c)$ electron density contoured at 1σ in the vicinity of zinc 1301 in the triclinic room-temperature structure of the dried crystal. The water molecule that completes the tetrahedral coordination sphere of zinc is colored pale blue. The pseudo-threefold axis of the hexamer is nearly parallel to the plane of the page. The densities at the zinc ion, the center of the imidazole rings and the water molecule are approximately 12, 4.5 and 3σ, respectively. Prepared with the programs *XtalView* (McRee, 1999) and *Raster3D* (Merritt & Bacon, 1997).

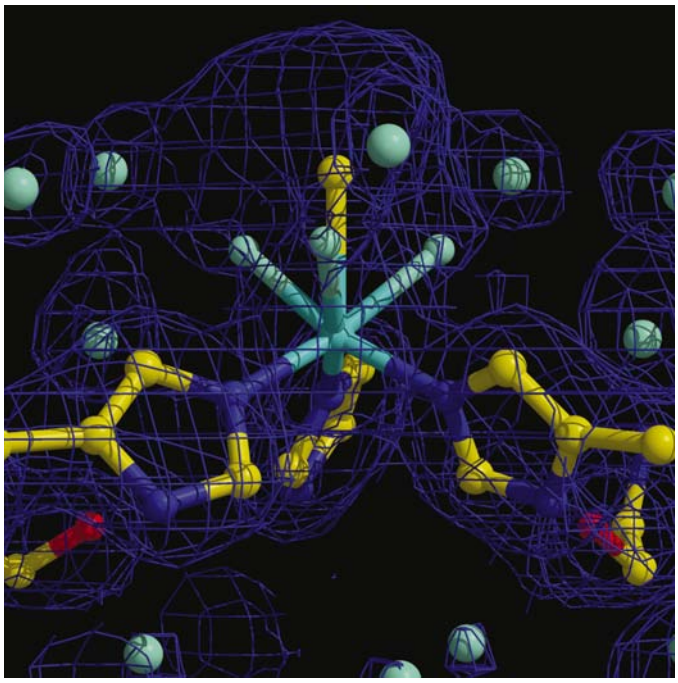

Figure 5
$(2F_o - F_c)$ electron density contoured at 1σ in the vicinity of zinc 501 in the trigonal 100 K structure illustrating the two alternate coordination schemes around the zinc ion. The three water molecules that complete the octahedral coordination sphere of zinc are colored pale blue, while the chloride ion that completes the tetrahedral coordination sphere is yellow. Also shown as pale blue spheres are water molecules that comprise a secondary hydration shell above the zinc ion. Prepared with the programs *XtalView* (McRee, 1999) and *Raster3D* (Merritt & Bacon, 1997).

residue and truncation of five additional residues to alanine. While the lack of completeness of the triclinic room-temperature data (83%) contributes to the poor quality of the maps, the thermal parameters in these portions of the A chains were considerably larger than in the remainder of the protein. The poor quality of the electron density in these regions, the large thermal motion, the displacements from the hydrated structure and the absence of an ordered water structure to stabilize the conformation all suggest that the A chains are disordered as a result of partial unfolding.

3.2. The 100 K structure

A C^{α} trace of the threefold-symmetric hexamer at 100 K in the rhombohedral setting is illustrated in Fig. 1. Unlike the room-temperature structure, the 100 K structure exhibited electron density that was well defined at both A-chain N-termini, even though the N-terminal A-chain mean-square atomic displacements were large relative to those of the remainder of the protein. However, the data completeness was approximately 100% and the $R_{\rm merge}$ (Table 1) was significantly smaller than that of the room-temperature data; these factors surely helped to improve the appearance of the electron densities.

Performing the least-squares alignment described above against PDB entry 4ins resulted in a mean displacement of 0.167 Å for the atoms used in the optimization and 0.374 Å for all backbone atoms. The largest individual displacements were observed at the N-terminus of the A chain of monomer 1 and at PheB1.2. Illustrated in Fig. 3 are the C^{α} displacements of the A chains relative to PDB entry 4ins. While the displacements of the C^{α} atoms of the first five residues of monomer 2 are small, those of monomer 1 are nearly as large as the displacements observed in the dried crystal at room temperature. The C^{α} of PheB1.2 is displaced 1.57 Å compared with 0.52 Å at PheB1.1. While this displacement at PheB1.2 is one of the larger displacements, it is still small compared with the 7.86 Å displacement observed in the structure of hydrated T_6 human insulin at 120 K (Smith *et al.*, 2003).

3.3. Zinc-ion coordination

In the room-temperature structure, each of the two zinc ions is coordinated by three $N^{\varepsilon 2}$ atoms from HisB10, with a mean Zn—N distance of 2.14 Å. Lying nearly on the pseudo-threefold axis of the hexamer and above each zinc ion is a large region of $(2F_o - F_c)$ electron density, illustrated in Fig. 4. These densities were modeled as water molecules with distances to the zinc ions of 2.30 and 2.64 Å, which results in tetrahedral coordination around zinc, although the second distance is rather long for a zinc ligand. No density even at 0.5σ was observed that might correspond to water molecules with octahedral coordination to zinc. It is entirely possible that the fourth tetrahedral coordination site may be partially occupied by a chloride ion with high thermal motion. A comparison of Figs. 4 and 5 shows that at room temperature there is an absence of electron density corresponding to the secondary hydration shell above the zinc ligands. In contrast, at 100 K the zinc-ion coordination, shown in Fig. 5, quite clearly indicates that there are two alternate coordination schemes around each zinc ion. Alternate or dual coordination for zinc has previously only been observed in T-state trimers in $T_3R_3^f$ hexameric insulin (Ciszak & Smith, 1994; Whittingham *et al.*, 1995; Smith *et al.*, 2001). The zinc ions, triply ligated by HisB10 $N^{\varepsilon 2}$ atoms, bind three water molecules and adopt octahedral coordination in one half of the zinc sites in the crystal; in the other half, the zinc ions adopt tetrahedral coordination, with the three water molecules replaced by a single chloride ion. The Zn—N distances were observed to be 2.05 and 2.01 Å, the Zn—Cl distances were 2.43 and 2.41 Å, and the Zn—water distances were 2.17 and 2.49 Å.

3.4. GluB13 residues in the hexamer central core

In T_6, $T_3R_3^f$ and R_6 insulin hexamers, three pairs of GluB13 side chains reside in the central core of the hexamer. While the side chains of these residues are frequently observed to occupy two discrete conformations in $T_3R_3^f$ and R_6 hexamers, no such disorder has been observed to date in T_6 hexamers. The results from the 1.5 Å resolution X-ray refinement (Baker *et al.*, 1988) and the joint 1.5 Å resolution X-ray and 2.2 Å resolution neutron refinement (Wlodawer *et al.*, 1989) of T_6 porcine insulin showed that the carboxylate O atoms of the two independent GluB13 side chains make a short contact of approximately 2.5 Å and that the carboxylate groups are suitably oriented for a hydrogen-bond interaction. However, because the crystal had been grown at a pH of approximately 6.5 and because there was no evidence for a proton (or deuteron) in the neutron density maps, it was concluded that the existence of a hydrogen bond could not be confirmed and a non-bonded interaction was suggested instead. A contact of 2.55 Å has also been observed in the 2.25 Å resolution structure of T_6 bovine insulin (Smith, Pangborn & Blessing, unpublished data). Based upon biophysical chemical evidence that indicates that the isoionic point of GluB13 is 6.4 (Kaarsholm *et al.*, 1990) and upon the observation of the 2.46 Å contact between independent $O^{\varepsilon 2}$ atoms in the 1.0 Å resolution structure of T_6 insulin at 120 K, Smith *et al.* (2003) suggested that a short strong centered carboxylate–carboxylic acid hydrogen bond links the pairs of independent GluB13 carboxylate groups, with a proton shared about equally between the pairs of partially charged $O^{\varepsilon 2}$ atoms.

In zinc-free cubic insulin, the asymmetric unit is a monomer and a crystallographic dyad generates the biologically relevant insulin dimer. At pH 5.0, a contact of approximately 2.8 Å was observed between pairs of crystallographically related GluB13 carboxylate groups (Diao, 2003). With increasing pH, the GluB13 side chain adopts a second conformation that separates the symmetry-related carboxylate groups. These results caused Diao (2003) to suggest that at the lower pH the carboxylate group is protonated and that the pK_a of GluB13 is higher than the normal value. Thus, the chemical behavior of the GluB13 carboxylate groups in dimeric insulin is very similar to that observed in T_6 hexameric insulin.

Table 3
Side-chain torsion angles for GluB13 residues in T_6 hexameric insulin in the present study and in PDB entries 4ins (Baker *et al.*, 1988), 3ins (Wlodawer *et al.*, 1989) and 1mso (Smith *et al.*, 2003).

PDB code	Monomer	χ^1 (°)	χ^2 (°)	χ^3 (°)
Dehydrated 295 K structure, 1os4	1	−59.0†	−69.1	−75.8
	2	−99.6†	53.7	−73.2
	3	−73.0‡	—	—
	4	−65.1	−56.3	75.3
	5	−59.0	−109.3	48.6
	6	−63.2	−55.6	85.0
Dehydrated 100 K structure, 1os3	1	−177.4§	—	—
	1	−72.4§	—	—
	2	−70.6¶	−70.7	−73.4
	2	−170.0¶	—	—
4ins	1	−69.1	−98.3	6.2
	2	−69.5	−106.2	2.2
3ins	1	−67.4	−98.5	12.7
	2	−75.0	−96.8	−6.7
1mso	1	−70.4	−77.6	−17.6
	2	−75.1	−81.8	−15.2

† The carboxylate group has an occupancy of 0.5. ‡ C^γ is present but the remainder of the chain is missing owing to disorder. § C^γ has two alternate conformations; the remainder of the side chain is missing owing to disorder. ¶ C^γ has two alternate conformations: in conformation 1, the remainder of the side chain has an occupancy of 0.5; in conformation 2, the remainder of the side chain is missing owing to disorder.

The GluB13 cluster and the $(2F_o - F_c)$ electron density in the dried crystal at room temperature are illustrated in Fig. 6. The electron density corresponding to the side chains of GluB13.4, GluB13.5 and GluB13.6 is well defined and these side chains were refined with occupancies of unity. The carboxylate groups of GluB13.5 and GluB13.6 are nearly parallel and point in opposite directions. The mean separation between the GluB13.5 and 13.6 carboxylate groups is 3.12 Å, with the two C^δ atoms separated by 3.03 Å and the two $O^{\varepsilon 2}$ atoms separated by 2.75 Å. This close O···O contact probably arises from errors in the χ^3 torsion angle of GluB13.5 and the orientation of the GluB13.5 and 13.6 carboxylate groups precludes a hydrogen-bonded interaction. The electron densities corresponding to the carboxylate groups of GluB13.1 and GluB13.2 were weak and these two carboxylate groups nearly interpenetrate ($O^{\varepsilon 1}$—$O^{\varepsilon 2}$ distance of 1.47 Å). Therefore, these two side chains were refined with occupancies of 0.5 so that when one of the carboxylate groups is in the modeled position, the other adopts multiple conformations resulting from rotations about χ^1, χ^2 and χ^3. No density was observed for the carboxylate group of GluB13.3, presumably because of disorder. The side-chain torsion angles of GluB13 in the room-temperature structure as well as in PDB entries 4ins (Baker *et al.*, 1988) and 3ins (Wlodawer *et al.*, 1989) are listed in Table 3.

In the hexamer in the dried crystal at 100 K, both the independent GluB13 side chains are disordered by χ^1 rotations of approximately 100°. The $(2F_o - F_c)$ electron density in the vicinity of the central core of the hexamer is illustrated in Fig. 7. No electron density was observed for either of the GluB13.1 carboxylate groups or for the second orientation of the GluB13.2 carboxylate group, which suggests that χ^2 and χ^3 adopt multiple values. The side-chain torsion angles of GluB13 in the 100 K structure are listed in Table 3.

3.5. Hydration state

It is well known that water structure contributes not only to the conformational stability of a protein but also to the integrity of its crystal structure, since most protein crystals do not survive even modest dehydration. The low-humidity monoclinic lysozyme structure maintained the same backbone conformation as its native structure, but the desiccated structure of crystal form IX of ribonuclease A exhibited substantial deviations from its native structure, some exceeding 5.0 Å. Accompanying these structural changes was a reduction in the unit-cell volume by 34%.

In the hydrated crystal structure of T_6 insulin, the shape of the hexamer is that of a flattened sphere, the flattened surfaces being perpendicular to the threefold axis of the hexamer. The hexamers are closely packed in the crystal and stabilized by numerous interhexamer contacts. This is illustrated schematically in Fig. 8: the A sites contain five residues and the B sites contain six residues which make nine A–B interhexamer contacts of less than 3.4 Å; four of these contacts are hydrogen bonds with donor–acceptor distances of less than 2.9 Å. Contacts between hexamers related by the *c*-axis translation involve 14 residues that make 21 contacts, six of which are hydrogen bonds.

Given such a tight packing of the hexamers in the crystal, it is not surprising that the volume of the unit cell does not change much as a result of drying and dehydration. A comparison of the unit-cell parameters of the dried crystal at room temperature and 100 K, of the hydrated crystal at 120 K (PDB entry 1mso) and of seven hydrated crystals at room temperature (Smith, Pangborn and Blessing, unpublished data) shows that the volumes change by less than 1% as a result of dehydration and by 4 and 5% as a result of cryocooling of the dehydrated and hydrated crystals, respectively.

Unfortunately, there is no way to accurately determine the amount of water that was retained by the air-dried crystal. T_6 porcine insulin contains 142 water molecules per insulin monomer or 31% water by weight (Baker *et al.*, 1988). Reference to five insulin structures determined in the resolution range 1.9–2.3 Å shows that on average 32 water molecules per monomer were identified, which is considerably more than were found in either the 2.25 Å resolution room-temperature structure or the 1.95 Å resolution 100 K structure of the present study.

Only 14 water molecules (∼2 per monomer) could be modeled reliably in the room-temperature structure and 12 of these lie on the hexamer surface. The mean $B_{\rm iso}$ of these 14 water molecules was 48.1 Å^2, compared with 42.5 Å^2 for the main-chain protein atoms. Because several peaks persisted in the $(2F_o - F_c)$ and $(F_o - F_c)$ electron-density maps, they were modeled as waters, even though they are farther than 3.4 Å from any protein atom. It is possible that these peaks correspond to counter-cations whose coordination sphere of water is disordered. Four water molecules in the structure of the dried crystal at room temperature are within 1.0 Å of the position of a corresponding water molecule in the T_6 porcine structure at room temperature structure (Baker *et al.*, 1988). In

many regions of the hexamer where one would normally expect to find ordered water, the $(2F_o - F_c)$ electron density was of poor quality and definition, particularly in the central core of the hexamer. At the same time, there was an absence of $(F_o - F_c)$ difference electron density that would normally be indicative of well defined water molecules. The appearance of the maps suggests that the water that remains within the lattice is severely disordered and is mixed with air that has diffused into the crystal. There was very little 1σ $(2F_o - F_c)$ density and no 3σ $(F_o - F_c)$ density in the water channels that are parallel to the c axis and coincident with the 3_1 and 3_2 screw axes, shown schematically in Fig. 8; this suggests that a considerable amount of air occupies these channels.

In the structure of the dried crystal at 100 K, 38 water molecules (19 per monomer) could be identified and, as was the case in the room-temperature structure, there was negligible electron density in the water channels parallel to the c axis. The mean $B_{\rm iso}$ for the water molecules was 44.6 Å^2, compared with 35.4 Å^2 for protein backbone atoms. 14 of the 38 water molecules were within 1.0 Å of the position of a water molecule in the fully hydrated T_6 human insulin structure at 120 K (Smith *et al.*, 2003). In the latter structure, 29 ordered water molecules were found in the central core of the insulin hexamer, arranged in three layers perpendicular to the crystallographic threefold axis. In the present study of the dried crystal at 100 K, six and seven water molecules were found that correspond to layer 1 and layer 3 water molecules, respectively, in the hydrated structure at 120 K, as illustrated in Fig. 9. As can be seen in Table 4, where contacts between water molecules in the central core in the present 100 K study and in the earlier 120 K structure are tabulated, four of the five water molecules are very close to their counterparts; however, water 606, which is colored cyan and lies near the edge of Fig. 9, is nearly midway between waters 645 and 649 in the hydrated hexamer. Also illustrated in Fig. 9 is the single independent hydrogen bond (2.66 Å between waters 622 and 624) in the central core of the 100 K structure of the dried crystal.

4. Conclusions

In solution studies of a monomeric insulin analog in which CysA6 and CysA11 were replaced by serine, the N-terminal A-chain α-helix was observed to undergo segmental unfolding, thus demonstrating the flexibility of this segment of the A chain (Hua *et al.*, 1996; Weiss *et al.*, 2000). The present room-temperature study of a dehydrated insulin crystal indicates that a well ordered water structure appears to be as important as the A6–A11 disulfide link in stabilizing an ordered conformation of the N-termini of the A chains. The electron densities in these regions in the dehydrated structure are very poor, suggesting that the N-terminal residues adopt multiple conformations as a result of partial unfolding. Other portions of the protein, such as the central A-chain segment, the central B-chain α-helix and the B-chain β-sheet, maintain their structural integrity and their electron densities are well defined.

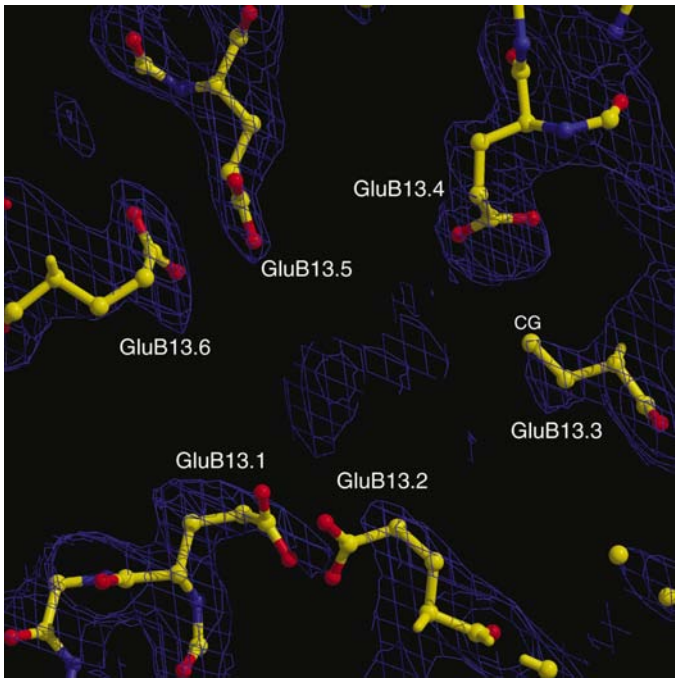

Figure 6
The 1σ-contoured σ_A-weighted $(2F_o - F_c)$ electron density in the central core of the T_6 insulin hexamer in the triclinic structure of the dehydrated crystal at room temperature. The view is along the hexamer's zinc–zinc axis, which corresponds to an approximate non-crystallographic threefold axis. The C^γ atom is labeled (CG) on GluB13.3, for which the carboxylate group is absent owing to disorder. Prepared with the programs *XtalView* (McRee, 1999) and *Raster3D* (Merritt & Bacon, 1997).

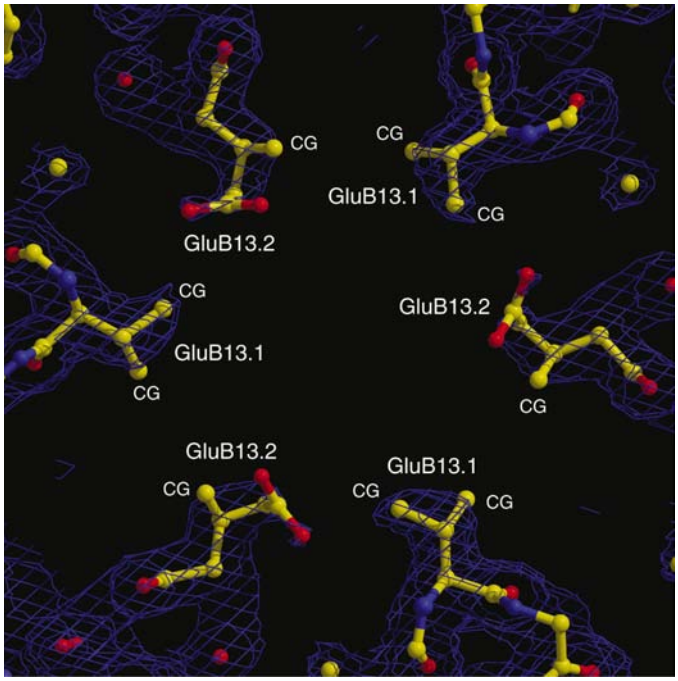

Figure 7
The 1σ-contoured σ_A-weighted $(2F_o - F_c)$ electron density in the central core of the T_6 insulin hexamer in the rhombohedral structure of the dehydrated crystal at 100 K. The view is along the crystallographic threefold axis. The C^γ atoms (CG) are labeled on those GluB13 residues which are incomplete owing to disordered carboxylate groups. Prepared with the programs *XtalView* (McRee, 1999) and *Raster3D* (Merritt & Bacon, 1997).

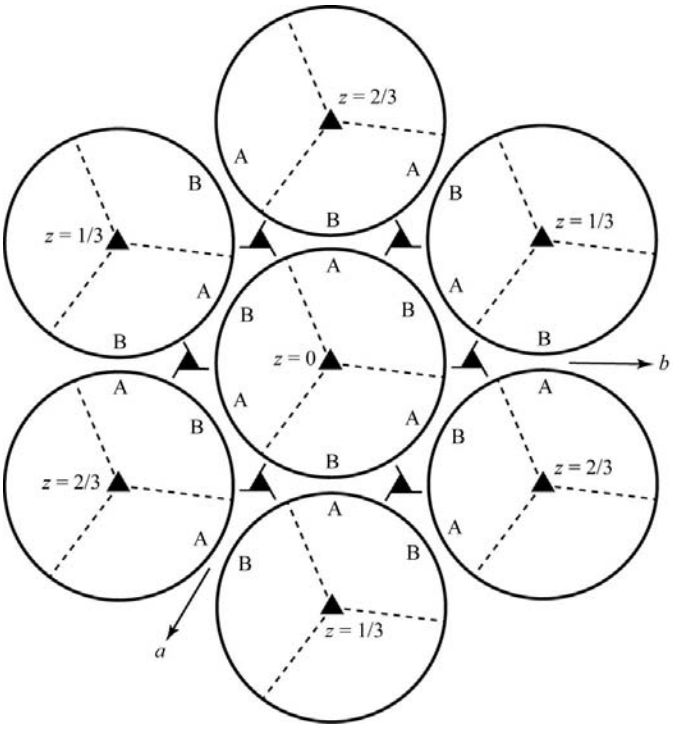

Figure 8
A schematic illustration of the packing of T_6 insulin hexamers in the hydrated *R*3 structure as viewed along the hexagonal *c* axis. Dashed lines denote the pseudo-twofold axes within the hexamers and the approximate boundary of each dimer. 'A' and 'B' label contact sites that contain five and six surface residues, respectively, that form nine interhexamer contacts of less than 3.4 Å, four of which are hydrogen bonds. Not shown are the contacts that exist between hexamers related by a translation along the *c* axis.

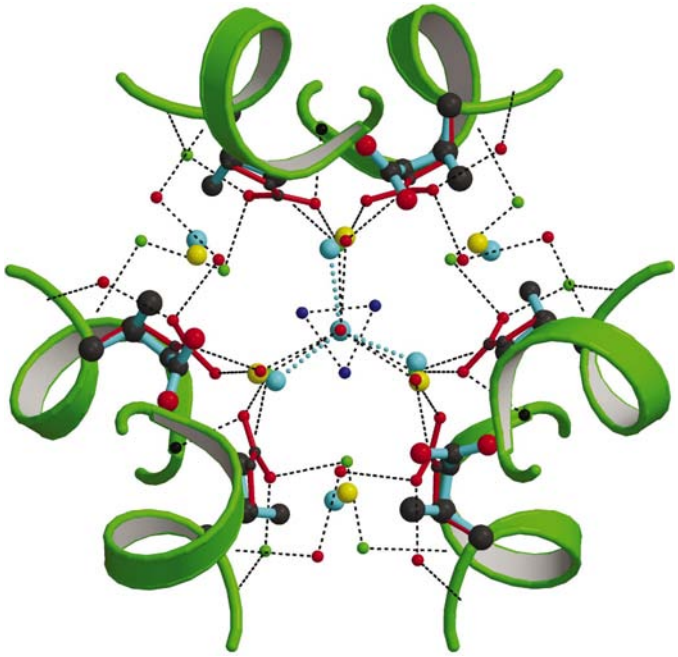

Figure 9
Water structure in the central core of the T_6 insulin hexamer in the 100 K dehydrated structure compared with that in the 120 K hydrated structure (PDB code 1mso). In the 120 K hydrated structure, all atoms and bonds are reduced in size and the color scheme is as follows: in water layers 1, 2 and 3 water molecules are red, blue and green, respectively; the GluB13 side chains are red and the black dotted lines represent hydrogen-bonded interactions. In the 100 K dehydrated structure, the B-chain segments are green, layer 1 and 3 water molecules are yellow and cyan, respectively, and bonds in the GluB13 side chains are cyan. The cyan dotted line represents the three symmetry-related hydrogen bonds between waters 624 and 622 in the 100 K dehydrated structure. Prepared with the programs *MOLSCRIPT* (Kraulis, 1991) and *Raster3D* (Merritt & Bacon, 1997).

At 100 K, the N-terminus of the A chain in monomer 2 in the dehydrated structure is properly folded and has a conformation that is nearly identical to that in the hydrated structure, but larger differences are observed in monomer 1. Small differences in conformation do exist between the two independent monomers, primarily in the first nine residues of the A chains, but these conformational differences are no larger than those observed in the hydrated structure at room temperature (PDB code 4ins). Unlike the dehydrated structure at room temperature, in which the N-termini of the A chains are partially disordered, the N-termini of the A chains at 100 K adopt ordered low-energy conformations, namely those of the hydrated structure.

A short ~2.5 Å $O^{\varepsilon 2}\cdots O^{\varepsilon 2}$ contact between independent GluB13 carboxylate groups has been observed in the T_6 hexameric forms of both porcine insulin at room temperature (Baker *et al.*, 1988; Wlodawer *et al.*, 1989) and human insulin at 120 K (Smith *et al.*, 2003). If, as was suggested by Wlodawer *et al.* (1989), neither of the independent GluB13 carboxylates is protonated, then the water structure in the central core of the hexamer would have to play a major role in dissipating six formal negative charges on the carboxylate groups and at the same time stabilize the conformations of the GluB13 side chains. If, on the other hand, as was reported by Kaarsholm *et al.* (1990), the pK_a of the GluB13 carboxylate groups has been modulated to approximately 6.4, then in crystals grown at pH 6.4 approximately half of the GluB13 carboxylate groups should be protonated. This would result in three hydrogen bonds amongst the six GluB13 side chains, which is consistent with the three short $O^{\varepsilon 2}\cdots O^{\varepsilon 2}$ contacts observed in hydrated T_6 insulin hexamers. It is also likely that the hexamer-core water structure is a factor in modulating of the pK_a of the GluB13 residues.

In both the room-temperature and 100 K dehydrated structures, there are no contacts between the GluB13 side chains that would suggest the presence of a hydrogen bond. In fact, severe disorder of these side chains is encountered in both structures and these are the first observed instances of GluB13 side-chain disorder in T_6 hexamers. In the absence of an ordered water structure, the GluB13 pK_a values presumably revert to normal values, resulting in six negative formal charges in the central core. To relieve charge-repulsion effects, the GluB13 side chains then become disordered in the manner we have observed in the dehydrated structures.

The authors thank Lilly Research Laboratories for a generous gift of biosynthetic human insulin, and Dr Marianna

Table 4
Distances between water molecules in the central core of the 100 K dehydrated structure and their counterparts in the 120 K hydrated structure.

Dehydrated residue No.	Hydrated residue No.	Distance (Å)
Layer 1		
610	630	0.73
628	624	0.35
Layer 2		
606	645	1.43
606	649	1.80
622	621	0.33
624	606	0.17

Long and Ms Vickie King of the Protein Crystallization Facility at the University of Alabama, Birmingham for setting up the microgravity crystal-growth experiments, which were supported by NASA grant NCC8-126 to Dr Lawrence J. DeLucas. Our research was supported by NIH grant GM56829. We thank an anonymous referee for a careful and helpful critique of an earlier version of this paper.

References

Adams, M. J., Blundell, T. L., Dodson, E. J., Dodson, G. G., Vijayan, M., Baker, E. N., Harding, M. M., Hodgkin, D. C., Rimmer, B. & Sheat, S. (1969). *Nature (London)*, **224**, 491–495.
Adams, P. D., Pannu, N. S., Read, R. J. & Brünger, A. T. (1997). *Proc. Natl Acad. Sci. USA*, **94**, 5018–5023.
Badger, J. (1993). *Biophys. J.* **65**, 1656–1659.
Baker, E. N., Blundell, T. L., Cutfield, J. F., Cutfield, S. M., Dodson, E. J., Dodson, G. G., Hodgkin, D. C., Hubbard, R. E., Isaacs, N. W., Reynolds, C. D., Sakabe, K., Sakabe, N. & Vijayan, N. M. (1988). *Philos. Trans. R. Soc. London, Ser. B*, **319**, 369–456.
Bell, J. A. (1999). *Protein Sci.* **8**, 2033–2040.
Bentley, G., Dodson, E., Dodson, G., Hodgkin, D. & Mercola, D. (1976). *Nature (London)*, **261**, 166–168.
Blessing, R. H. (1997). *J. Appl. Cryst.* **30**, 421–426.
Blessing, R. H. (1999). *Lecture Notes, Crystallographic Computing School on Frontiers in Computational Crystallography*, Hinxton, Cambridge, England, August 1999.
Blessing, R. H., Guo, D. Y. & Langs, D. A. (1998). *Direct Methods for Solving Macromolecular Structures*, *NATO ASI Series C: Mathematical and Physical Sciences*, Vol. 507, edited by S. Fortier, pp. 47–71. Dordrecht, The Netherlands: Kluwer Academic Publishers.
Brünger, A. T. (1992). *Nature (London)*, **355**, 472–474.
Brünger, A. T., Adams, P. D., Clore, G. M., DeLano, W. L., Gros P., Grosse-Kunstleve, R. W., Jiang J., Kuszewski, J., Nilges, M., Pannu, N. S., Read, R. J., Rice, L. M., Simonson, T. & Warren, G. L. (1998). *Acta Cryst.* D**54**, 905–921.
Brünger, A. T., Adams, P. D. & Rice, L. M. (1997). *Structure*, **5**, 325–336.
Ciszak, E., Beals, J. M., Frank, B. H., Baker, J. C., Carter, N. D. & Smith, G. D. (1995). *Structure*, **3**, 615–622.
Ciszak, E. & Smith, G. D. (1994). *Biochemistry*, **33**, 1512–1517.
DeLano, W. L. & Brünger, A. T. (1995). *Acta Cryst.* D**51**, 740–748.
Derewenda, U., Derewenda, Z., Dodson, E. J., Dodson, G. G., Reynolds, C., Sparks, K., Smith, G. D. & Swenson, D. C. (1989). *Nature (London)*, **338**, 594–596.
Diao, J. (2003). *Acta Cryst.* D**59**, 670–676.
Dung, M. H. & Bell, J. A. (1997). *Acta Cryst.* D**53**, 419–425.
French, S. & Wilson, K. (1978). *Acta Cryst.* A**34**, 517–525.
Heras, B., Edeling, M. A., Byriel, K. A., Jones, A., Raina, S. & Martin, J. L. (2003). *Structure*, **11**, 139–145.
Hua, Q.-X., Hu, S.-Q., Frank, B. H., Jia, W., Chu, Y.-C., Wang, S.-H, Burke, G. T., Katsoyannis, P. G. & Weiss, M. A. (1996). *J. Mol. Biol.* **264**, 390–403.
Kaarsholm, N. C., Havelund, S. & Hougaard, P. (1990). *Arch. Biochem. Biophys.* **283**, 496–502.
Kaarsholm, N. C., Ko, H. & Dunn, M. F. (1989). *Biochemistry*, **28**, 4427–4435.
Kraulis, P. (1991). *J. Appl. Cryst.* **24**, 946–950.
Laskowski, R. A., MacArthur, M. W., Moss, D. S. & Thornton, J. M. (1993). *J. Appl. Cryst.* **26**, 283–291.
McRee, C. E. (1999). *J. Struct. Biol.* **125**, 156–165.
Madhusudan, Kodandapani, R. & Vijayan, M. (1993). *Acta Cryst.* D**49**, 234–245.
Merritt, E. A. & Bacon, D. J. (1997). *Methods Enzymol.* **277**, 505–524.
Pannu, N. S. & Read, R. J. (1996). *Acta Cryst.* A**52**, 659–668.
Pflugrath, J. W. (1999). *Acta Cryst.* D**55**, 1718–1725.
Read, R. J. (1986). *Acta Cryst.* A**42**, 140–149.
Rice, L. M. & Brünger, A. T. (1994). *Proteins Struct. Funct. Genet.* **19**, 277–290.
Sack, J. S. (1988). *J. Mol. Graph.* **6**, 244–245.
Schlichtkrull, J. (1958). *Insulin Crystals.* Copenhagen: Munksgaard.
Smith, G. D. (1993). *PROFIT. A Locally Written Program for Orienting one Protein Molecule onto Another by a Least-Squares Procedure.* Hauptman–Woodward Medical Institute, Buffalo, USA.
Smith, G. D., Pangborn, W. A. & Blessing, R. H. (2001). *Acta Cryst.* D**57**, 1091–1100.
Smith, G. D., Pangborn, W. A. & Blessing, R. H. (2003). *Acta Cryst.* D**59**, 474–482.
Weiss, M. A., Hua, Q.-X., Jia, W., Chu, Y.-C., Wang, R.-Y. & Katsoyannis, P. G. (2000). *Biochemistry*, **39**, 15429–15440.
Whittingham, J. L., Chaudhurri, S., Dodson, E. J., Moody, P. C. E. & Dodson, G. G. (1995). *Biochemistry*, **34**, 15553–15563.
Wlodawer, A., Savage, H. & Dodson, G. (1989). *Acta Cryst.* B**45**, 99–107.